ORIGINAL RESEARCH

MAGOH/MAGOHB Inhibits the Tumorigenesis of Gastric Cancer via Inactivation of b-RAF/MEK/ERK Signaling

Yong Zhou[1,*]
Zhongqi Li[1,*]
Xuan Wu[1]
Laizhen Tou[1]
Jingjing Zheng[2]
Donghui Zhou[1]

[1]Department of Oncology, First Affiliated Hospital, Zhejiang University School of Medicine, Hangzhou 310003, People's Republic of China; [2]Department of General Surgery, Lishui Municipal Central Hospital, Lishui, Zhejiang 323000, People's Republic of China

*These authors contributed equally to this work

Background: Gastric cancer is one of the most malignant tumors all over the world. It has been reported that proteins play key roles during the tumorigenesis of gastric cancer. To identify novel potential targets for gastric cancer, differential expressed proteins between gastric cancer and adjacent normal tissues were analyzed with proteomics and bioinformatics tool.

Methods: The differentially expressed proteins between gastric cancer and adjacent normal tissues were analyzed by Omicsbean (multi-omics data analysis tool). Cell viability was tested by CCK-8 assay. Flow cytometry was used to measure cell apoptosis and cycle. Transwell assay was used to test cell migration and invasion. Gene and protein expressions were detected by RT-qPCR, immunohistochemistry and Western blot, respectively.

Results: MAGOH and MAGOHB were found to be notably upregulated in gastric cancer tissues compared with that in normal tissues. Knockdown of MAGOH significantly inhibited the proliferation of gastric cancer cells via inducing the cell apoptosis. In addition, MAGOH knockdown induced G2 phase arrest in gastric cancer cells. Moreover, MAGOH knockdown notably inhibited migration and invasion of gastric cancer cells. Importantly, double knockdown of MAGOH and MAGOHB exhibited much better anti-tumor effects on gastric cancer compared with alone treatment. Finally, double knockdown of MAGOH and MAGOHB mediated the tumorigenesis of gastric cancer via regulation of RAF/MEK/ERK signaling.

Conclusion: MAGOH knockdown inhibited the tumorigenesis of gastric cancer via mediation of b-RAF/MEK/ERK signaling, and double knockdown of MAGOH and MAGOHB exhibited much better anti-tumor effects. This finding might provide us a new strategy for the treatment of gastric cancer.

Keywords: gastric cancer, MAGOH/MAGOHB, b-RAF/MEK/ERK signaling

Introduction

Gastric cancer (GC) is one of the leading causes of cancer-related death worldwide with high rates of mortality.[1,2] Nowadays, the main treatments of GC include surgery and chemotherapy.[3] Despite the efforts that have been made, the overall survival rate of patients with GC has not improved greatly.[4] Although many molecular targets have been confirmed to be involved in the progression of GC,[5] the study of GC remains to be further explored.

MAGOH (mago-nashi homolog) is a key component of the exon junction complex (EJC), which mediates mRNA processing (splicing, translation, and localization).[6] In addition, MAGOH is known to be part of a conserved syntenic

Correspondence: Donghui Zhou
Department of Oncology, First Affiliated Hospital, Zhejiang University School of Medicine, Hangzhou, Zhejiang 310003, People's Republic of China,
Email 1193076@zju.edu.cn

group in vertebrates exclusively.[7] Meanwhile, MAGOH is involved in various kinds of malignant tumors.[8–10] For example, Stricker et al found MAGOH was upregulated in breast cancer.[10] On the other hand, MAGOHB is the duplicated MAGOH gene which is the top gene dependency in cells with hemizygous MAGOH deletion (a pervasive genetic event that frequently occurs due to chromosome 1p loss).[11] Inhibition of MAGOHB in a MAGOH-deleted context compromises viability by globally perturbing alternative splicing and RNA surveillance.[12]

In this study, proteomics and bioinformatics analysis were used to identify the differentially expressed protein between gastric cancer tissues and adjacent normal tissues. We found MAGOH and MAGOHB were notably upregulated in gastric cancer tissues compared with that in normal tissues. Moreover, the functions of MAGOH and MAGOHB in gastric cancer were explored.

Materials and Methods
Cell Culture
The GC cell lines (BGC823, AGS, SGC-7901 and HGC27) and human gastric mucosal cell line (GES-1) were obtained from the State Key Laboratory for Diagnosis and Treatment of Infectious Diseases, the First Affiliated Hospital, Zhejiang University School of Medicine. Cells were cultured in RPMI 1640 supplemented with 10% fetal bovine serum (FBS), 100 μg/mL streptomycin and penicillin at 37°C in 5% CO_2. The use of cells was approved by the Ethics Committee of Zhejiang University School of Medicine (20,190,711).

Tissue Collection
Thirty gastric cancer tissues and 25 adjacent tumor tissues were obtained from patients who were diagnosed with gastric cancer for the first time and underwent surgical resection. Gastric cancer tissues and adjacent normal tissues of all patients were collected and stored at −80°C. All participants have signed written informed consent. This study was in line with the Helsinki Declaration and has been approved by the Ethics Committee of Zhejiang University School of Medicine (20,190,405). The clinical information of patients was presented in supplementary information.

Vector Construction and Cell Transfection
The human MAGOH siRNA (10 nM), MAGOHB siRNA (10 nM) and the corresponding siRNA control (referred to as NC) were purchased from Sangon Biotech Co., Ltd (Shanghai, China). Next, MAGOH siRNA and MAGOHB siRNA were transfected into gastric cancer cells using Lipofectamine® 2000 (Thermo Fisher Scientific) according to the manufacturer's instructions. The efficiency of transfection was detected by reverse transcription-quantitative PCR (RT-qPCR) and Western blot. The sequences of siRNAs: NC siRNA, UUCUCCGAACGUGUCACGUTT; MAGOH siRNA,GCGUGAUGGAGGAACUGAATT; MAGOHB siRNA,GGCUGUUUGUAUAUUUAAUTT.

CCK-8 Assay
Cell counting kit-8 assay (CCK8; Beyotime Institute of Biotechnology) was used to investigate cell proliferation. Gastric cancer cells were plated into 96-well plates with a density of $5×10^3$ cells per well and treated with negative control (NC), MAGOH siRNA, MAGOHB siRNA or MAGOH siRNA + MAGOHB siRNA (siMAGOH+B) for 0, 1, 2, 3, 4, 5 or 6 days, respectively. Cells were then incubated with 10 μL CCK-8 reagent (Beyotime, Shanghai, China) for another 2 h at 37°C. Subsequently, the absorbance of cells was measured at 450 nm using a microplate reader (Thermo Fisher Scientific).

Colony Formation Assay
Gastric cells were seeded in 12-well plates in DMEM in triplicate (100 cells/well) and transfected with NC siRNA, MAGOH siRNA, MAGOHB siRNA or MAGOH+B siRNA. Next, the plates were maintained in a 37°C incubator for 14 days and the colonies that contained more than 50 cells were fixed with pre-iced methanol for 10 min at room temperature. Then, the colonies were stained with crystal violet (1%) for 5 min at room temperature. Finally, the number of colonies was counted under a light microscope (Nikon, Tokyo, Japan) at a magnification of ×200.

Transwell Assay
Transwell plates (24-well, Corning, New York, NY, USA) were used for cell invasion and migration detection. For the cell migration assay, $2×10^5$ BGC-823 cells were seeded into the upper chambers of plates in 200 μL RPMI 1640 medium

supplemented with 0.2% FBS. The lower chambers contained RPMI 1640 medium supplemented with 1% FBS. After 24 h of incubation at 37°C, the non-migrating cells were gently removed from the upper side of chamber with a cotton swab, while the cells that migrated into underside of the membrane were fixed with 95% alcohol for 10 min and stained with 1% crystal violet (Sigma, Grand Island, NY, USA) for 5 min. Finally, images were captured, and the cells were counted under an inverted light microscope (Olympus) at 400x magnification.

For the invasion assay, the upper chambers of plates were pretreated with 50 μL of Matrigel (12.5 mg/L, BD Biosciences, Franklin Lake, NJ, USA) overnight. Then, BGC-823 cells (1×10^6 cells/mL) in FBS-free medium were seeded into the upper chambers. The lower chambers contained RPMI 1640 medium supplemented with 1% FBS. The cells were incubated at 37°C for 24 h, and cells that had attached to the underside of the membrane were fixed and stained with a 0.1% crystal violet solution. Finally, images were captured, and the number of invading cells was counted under a microscope at 400x magnification.

Cell Apoptosis
Gastric cancer cells were seeded in 6-well plate. The cells were harvested by centrifuging at 300 g for 5 min and the residue was resuspended with 100 μL binding buffer. Then, 5 μL Annexin V-FITC and 5 μL propidium (PI) were added in the dark for 15 min. The cell apoptotic rate was measured by flow-cytometer (BD, Franklin Lake, NJ, USA).

Quantitative Real-Time Polymerase Chain Reaction (RT-qPCR)
Total RNAs were extracted from tissues or cell lines with TRIZOL reagent (Invitrogen, Carlsbad, CA, USA). We carried out reverse transcription and real-time PCR with PrimeScript RT reagent Kit (Takara, Tokyo, Japan) and SYBR premix Ex Taq II kit (Takara, Tokyo, Japan), respectively. GAPDH was used as the internal control. The sequences of primers are listed in Table 1. $2^{-\Delta\Delta CT}$ method was utilized to measure the relative gene expression.

Bioinformatics Analysis
The differentially expressed proteins between GC and adjacent normal tissues were identified by Omicsbean (multi-omics data analysis tool). Biological pathways were defined by Omicsbean (http://www.omicsbean.cn/).

Table 1 The Sequences of Primers

Gene	Sequence of Primer
MAGOH	Forward: 5-GACCGGACGGGAAGTTAAGA-3
	Reverse: 5-TTCAGTTCCTCCATCACGCTT-3
MAGOHB	Forward: 5-GCGATTTCTACCTGCGCTAC-3
	Reverse: 5-GAGGCCACAAAGCATCATCT-3
GAPDH	Forward: 5-GAACATCATCCCTGCCTCTACT-3
	Reverse: 5-ATTTGGCAGGTTTTTCTAGACG-3

Western-Blot Detection
Total protein was isolated from cell lysates or tumor tissues with RIPA buffer, and quantified by BCA protein assay kit (Beyotime, Shanghai, China). Proteins were resolved on 10% SDS-PAGE and then transferred into PVDF (Bio-Rad) membranes. After blocking with 5% skim milk for 1 h, the membranes were incubated with primary antibodies at 4°C overnight. Then, membranes were incubated with secondary anti-rabbit antibody (Abcam; 1:5000) at room temperature for 1 h. After that, membranes were scanned by using an Odyssey Imaging System and analyzed with Odyssey v2.0 software (LICOR Biosciences, Lincoln, NE, USA). The primary antibodies used in this study were as follows: anti-MAGOH (Abcam, Cambridge, MA, USA; 1:1000), anti-MAGOHB (Abcam; 1:1000), anti-ERK (Abcam; 1:1000), anti-p-ERK (Abcam; 1:1000), anti-mTOR (Abcam; 1:1000), anti-RAF-b (Abcam; 1:1000), anti-MEK (Abcam; 1:1000), anti-cleaved caspase 3 (Abcam; 1:1000), anti-Cyclin B1 (Abcam; 1:1000), anti-p27 Kip1 (Abcam; 1:1000) and anti-CDK1 (Abcam; 1:1000). GAPDH was used as an internal control.

Immunohistochemistry (IHC)
Tumor tissues obtained from patients with gastric cancer were fixed with 10% formaldehyde solution and then embedded in paraffin to cut into sections with a thickness of 3 μm. After dehydration by xylene and gradient alcohol, the sections were subjected to antigen retrieval using citrate buffer (pH=6.0) for 30 min. H_2O_2 (3%) was used to incubate these sections in order to remove endogenous peroxidase. Then the sections were blocked with goat serum for 15 min and incubated with MAGOH/MAGOHB primary antibodies (Abcam; 1:1000) at 4°C overnight, followed by incubated with HRP-labeled secondary antibodies (Abcam; 1:5000) for 15 min at 37°C. At last, the section was sealed with neutral resin and observed under a microscope. The histochemistry score (H-score) was calculated as follows: (percentage of weak intensity ×1) +
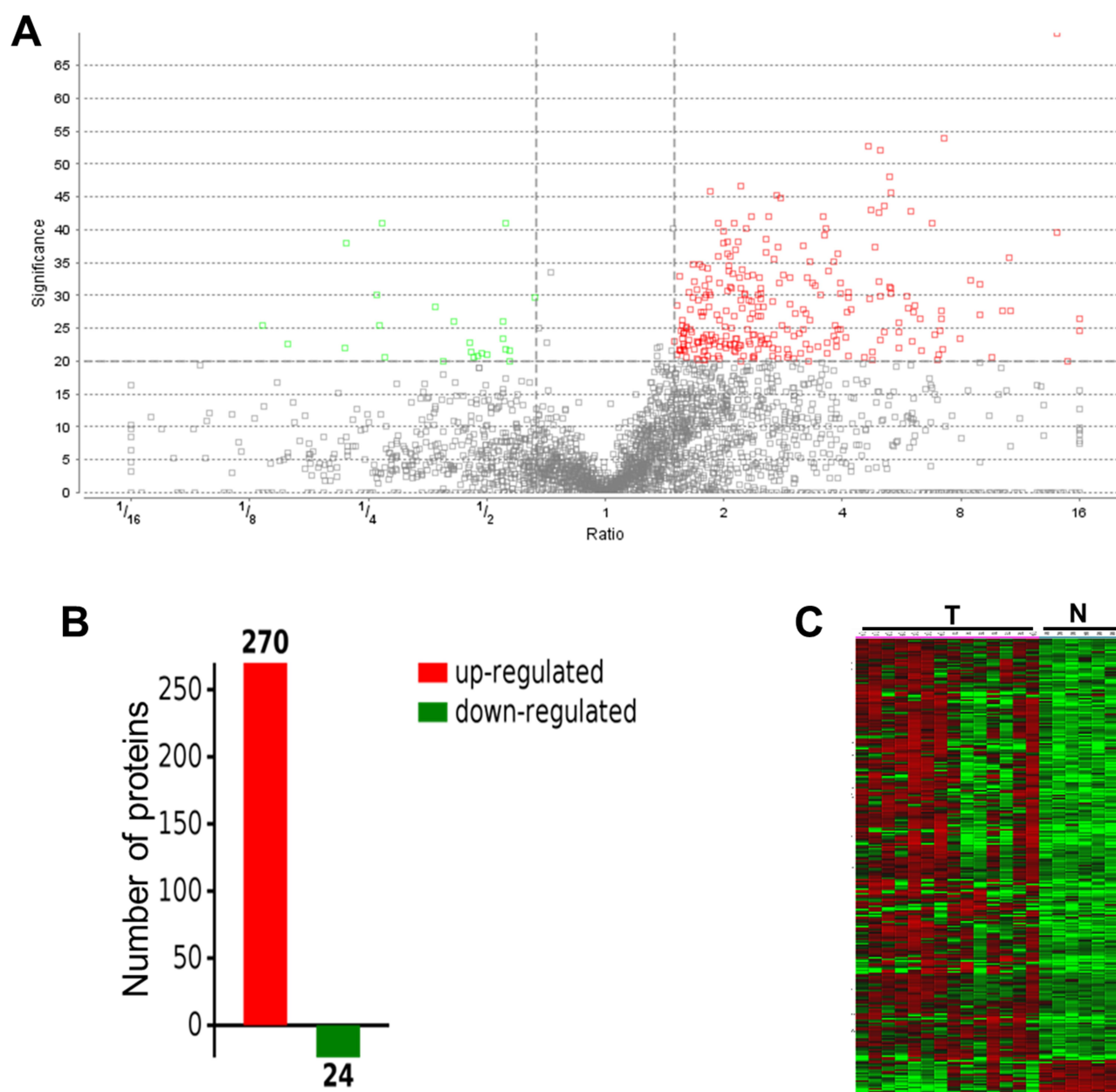
Figure 1 Differentially expressed proteins in gastric cancer were presented. (**A** and **B**) A total of 294 differentially expressed proteins between gastric cancer and normal tissues were presented by volcano map. Among these differentially expressed proteins in proteomics, 270 were significantly upregulated in gastric cancer, whereas 24 were downregulated. (**C**) Differentially expressed proteins among tumor tissues and adjacent normal tissues were presented in heatmap.

(percentage of moderate intensity ×2) + percentage of strong intensity ×3.[13]

Cell Cycle Detection

Cell cycle was determined by flow cytometry using Cycle Detection Kit I (BD Biosciences, Franklin Lake, NJ, USA). Gastric cancer cells were seeded in 6-well plate one day before cell transfection. After 24 h of transfection,

the cells were collected and fixed in pre-cold 70% ethanol at 4°C overnight. Then, cells were treated with 100 μL PI/ RNase Staining Buffer (Thermo Fisher Scientific, Waltham, MA, USA) at room temperature in the dark for 30 min. Finally, Flow cytometry (BD Biosciences, Franklin Lake, NJ, USA) was used to detect the cell cycle distribution and the data was analyzed with the Flowjo software (BD, Franklin Lake, NJ, USA).
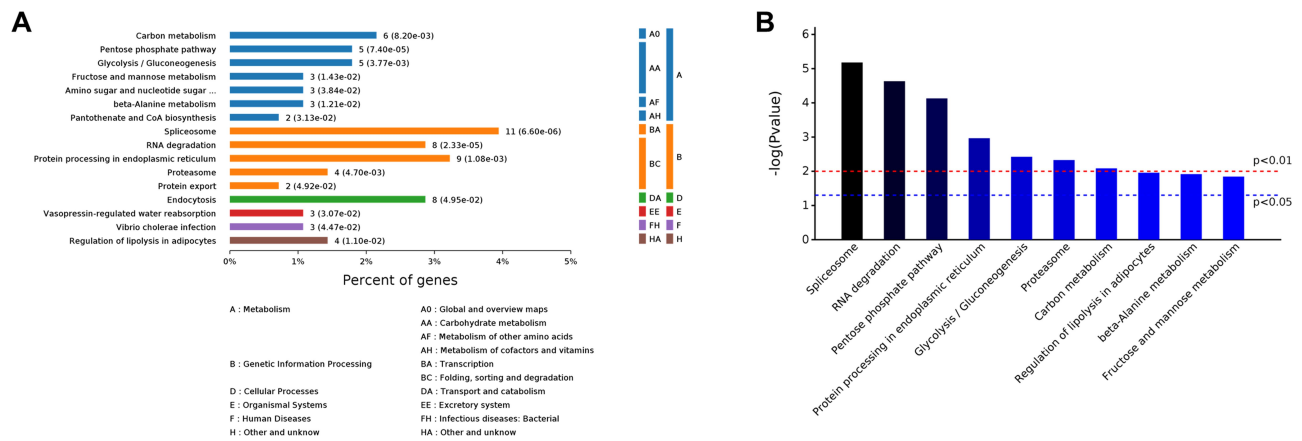
Figure 2 Cellular functions of differentially expressed proteins were analyzed with Omicsbean. (**A**) The potential functions of differentially expressed proteins were investigated by Omicsbean. (**B**) The signaling pathways related to differentially expressed proteins were presented by Omicsbean.

Statistical Analysis

Data are presented as the mean ± SD. The comparison between two groups was analyzed using Student's t-test. Comparisons among multiple groups were made using ANOVAs followed by Tukey's test using the Graphpad Prism 7 (GraphPad Software, Inc.). P < 0.05 was considered to indicate a statistically significant difference.
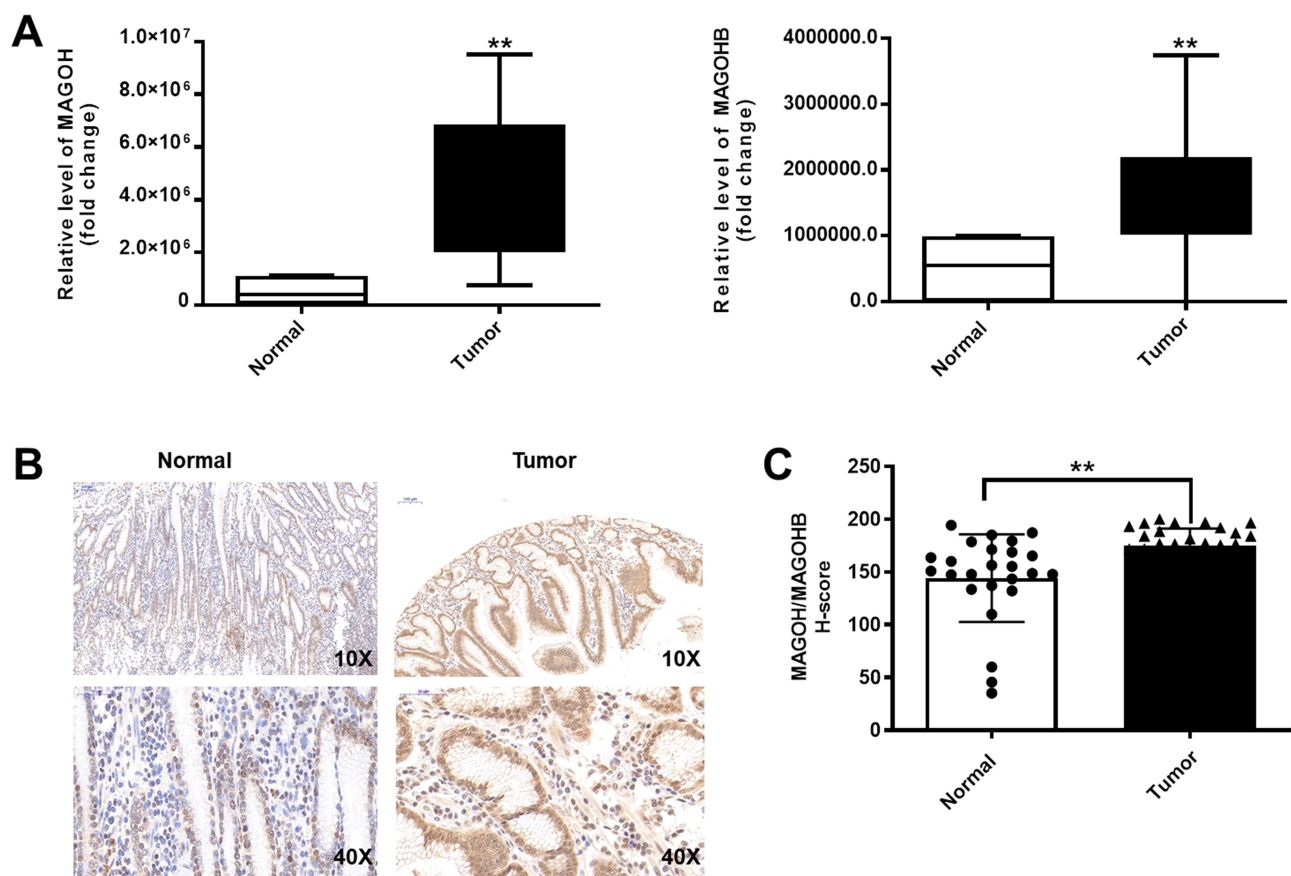

Figure 3 MAGOH and MAGOHB were significantly upregulated in gastric cancer tissues. (**A**) The expressions of MAGOH and MAGOHB in gastric cancer tissues or adjacent normal tissues were detected by RT-qPCR. (**B**) The protein expressions of MAGOH and MAGOHB in gastric cancer tissues or in adjacent normal tissues were detected by IHC. (**C**) IHC H-score was calculated. **P < 0.01 compared to normal tissues.
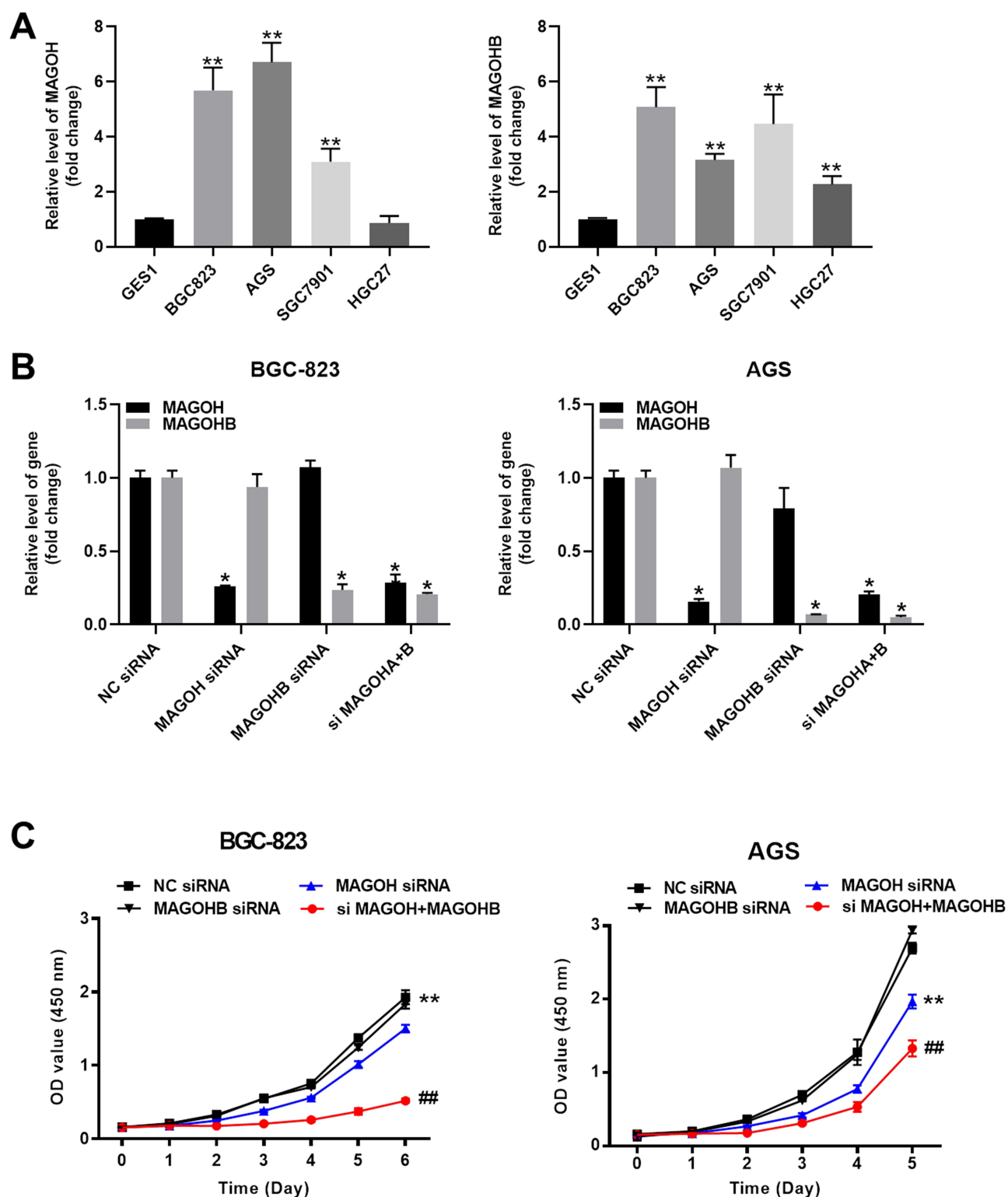
Figure 4 Knockdown of MAGOH or double knockdown of MAGOH and MAGOHB significantly inhibited the cell viability of gastric cancer. (**A**) The expressions of MAGOH and MAGOHB in gastric cancer cells or in human gastric mucosal cells were detected by RT-qPCR. (**B**) The expressions of MAGOH and MAGOHB in AGS or BGC-823 cells were detected by RT-qPCR. (**C**) BGC-823 or AGS cells were treated with siRNA control, MAGOH siRNA, MAGOHB siRNA or MAGOH siRNA + MAGOHB siRNA (si MAGOH+B). Then, cell viability was tested by CCK-8 assay. *P < 0.05, **P < 0.01, **P < 0.01 compared to GES-1 or NC siRNA. ##P < 0.01 compared to MAGOH siRNA.
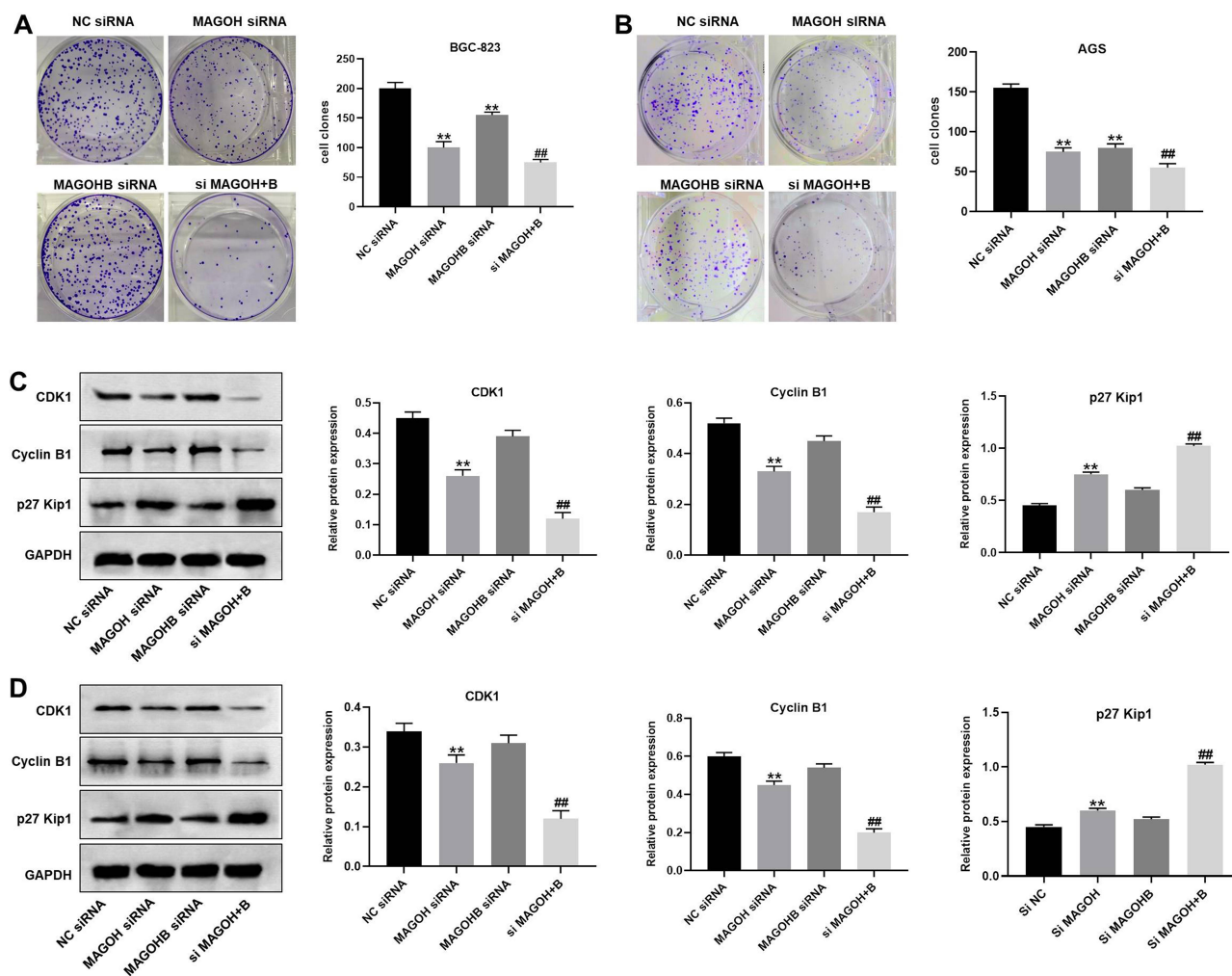
Figure 5 Knockdown of MAGOH or double knockdown of MAGOH and MAGOHB inhibited the proliferation of gastric cancer cells via regulation of CDK1, Cyclin B1 and p27 Kip1. (**A**) The clones of BGC-823 cells were detected by colony formation assay. (**B**) The clones of AGS cells were detected by colony formation assay. (**C** and **D**) The protein expressions of Cyclin B1, CDK1 and p27 Kip1 in gastric cancer cells were detected by Western blot. The relative expressions were quantified by normalizing to GAPDH. **P <0.01 compared to NC siRNA. ##P < 0.01 compared to MAGOH siRNA.

Results

Differentially Expressed Proteins Between Gastric Cancer Tissues and Normal Tissues Were Analyzed with Omicsbean

To explore the differentially expressed proteins between gastric cancer and adjacent normal tissues, Omicsbean was used. As indicated in Figure 1A–C, 294 differentially expressed proteins in gastric cancer were found. Among these differentially expressed proteins in proteomics, 270 were significantly upregulated in gastric cancer compared with that in normal tissues, whereas 24 were downregulated. Additionally, the data from Omicsbean revealed that the most enriched cellular process was apoptosis and the most enriched genetic information processing was spliceosome.

Meanwhile, the most enriched environmental information processing was AMPK signaling pathway (Figure 2A). In addition, RNA synthesis, splicing and metabolism were closely correlated with tumorigenesis of gastric cancer (Figure 2B). Based on these data, MAGOH and MAGOHB were selected for further investigations.

MAGOH and MAGOHB Were Notably Upregulated in Gastric Cancer Tissues

In order to detect the gene expressions, RT-qPCR was performed. As illustrated in Figure 3A, both MAGOH and MAGOHB were significantly upregulated in gastric cancer tissues, compared with that in adjacent normal tissues. Consistently, H-score of MAGOH or MAGOHB in gastric cancer tissues was notably increased, compared to normal tissues (Figure 3B and C). All these results
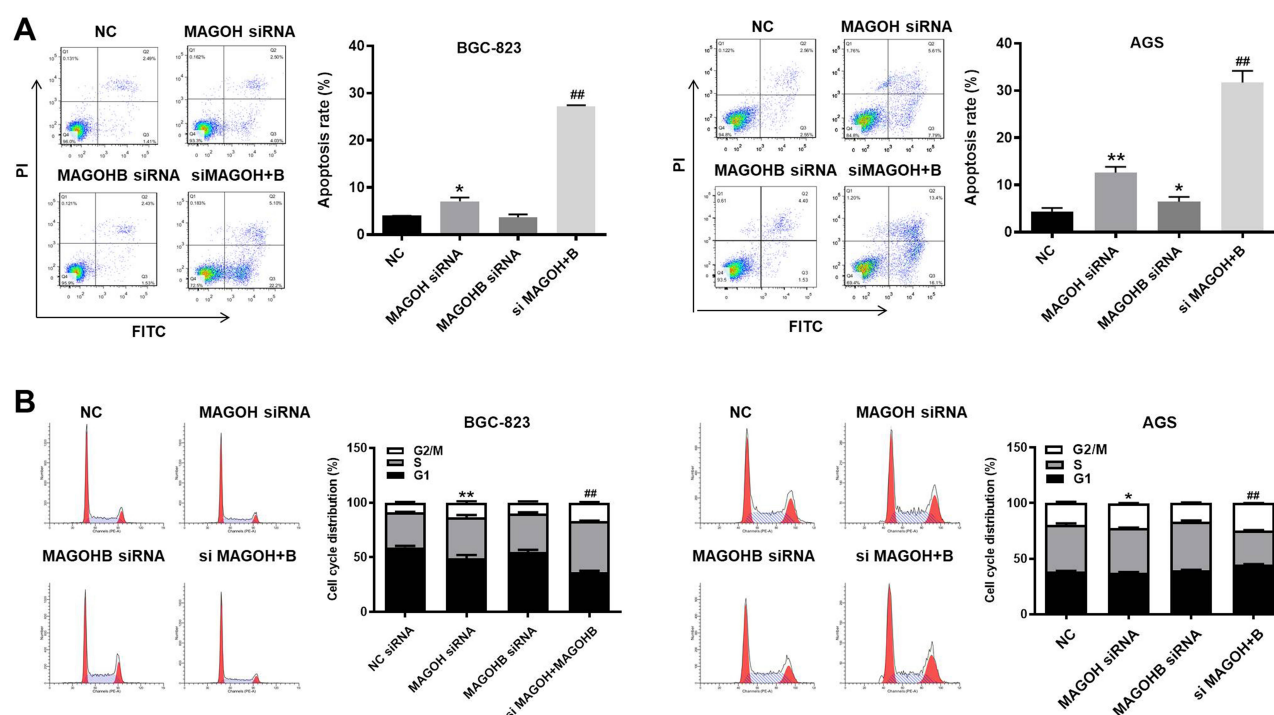
Figure 6 Knockdown of MAGOH or double knockdown of MAGOH and MAGOHB significantly inhibited the growth of gastric cancer cells. (**A**) Cell apoptosis was detected with Annexin V/PI staining. The rate of apoptotic cells was detected by FACS. X axis: the level of Annexin-V FITC fluorescence; Y axis: the PI fluorescence. (**B**) The cell cycle distribution (G0/G1, S, and G2 phase) in gastric cancer cells were determined by FACS. *P < 0.05, **P < 0.01 compared to NC. ##P < 0.01 compared to MAGOH siRNA.

demonstrated that both MAGOH and MAGOHB were upregulated in gastric cancer tissues.

Knockdown of MAGOH or double knockdown of MAGOH and MAGOHB Inhibited the Viability of Gastric Cancer Cells

For the purpose of investigating the gene expression of MAGOH and MAGOHB in gastric cancer cells, RT-qPCR was used. As shown in Figure 4A, both MAGOH and MAGOHB were notably upregulated in gastric cancer cells, compared with GES-1 cells. Since MAGOH expression in BGC823 and AGS cells was higher than other two gastric cancer cell lines, BGC823 and AGS cell lines were selected for use in the following experiments. Next, MAGOH siRNA or MAGOHB siRNA was stably transfected into gastric cancer cells (Figure 4B), and cell viability of gastric cancer was significantly inhibited by MAGOH siRNA. Importantly, the combination of MAGOH siRNA with MAGOHB siRNA exhibited much better anti-proliferation effect compared with alone treatment (Figure 4C). Taken together, knockdown of NAGOH or double knockdown of MAGOH and MAGOHB

inhibited the viability of gastric cancer cells and double knockdown of MAGOH and MAGOHB exhibited much better anti-proliferation effect.

Knockdown of MAGOH or double knockdown of MAGOH and MAGOHB Inhibited the Colony Formation of Gastric Cancer Cells via Regulation of CDK1, Cyclin B1 and P27 Kip1

To further detect the effect of MAGOH siRNA or MAGOHB siRNA on cell proliferation, cell colony formation assay was performed. As indicated in Figure 5A and B, the proliferation of gastric cancer cells was significantly inhibited by MAGOH siRNA, and this phenomenon was further aggravated by the combination treatment. Meanwhile, knockdown of MAGOH or double knockdown of MAGOH and MAGOHB notably downregulated the expressions of CDK1 and cyclin B1 and increased the level of p27 Kip1 in gastric cancer cells (Figure 5C and D). Taken together, knockdown of MAGOH or double knockdown of MAGOH and MAGOHB inhibited the proliferation of gastric cancer cells via regulation of CDK1, Cyclin B1 and p27 Kip1.
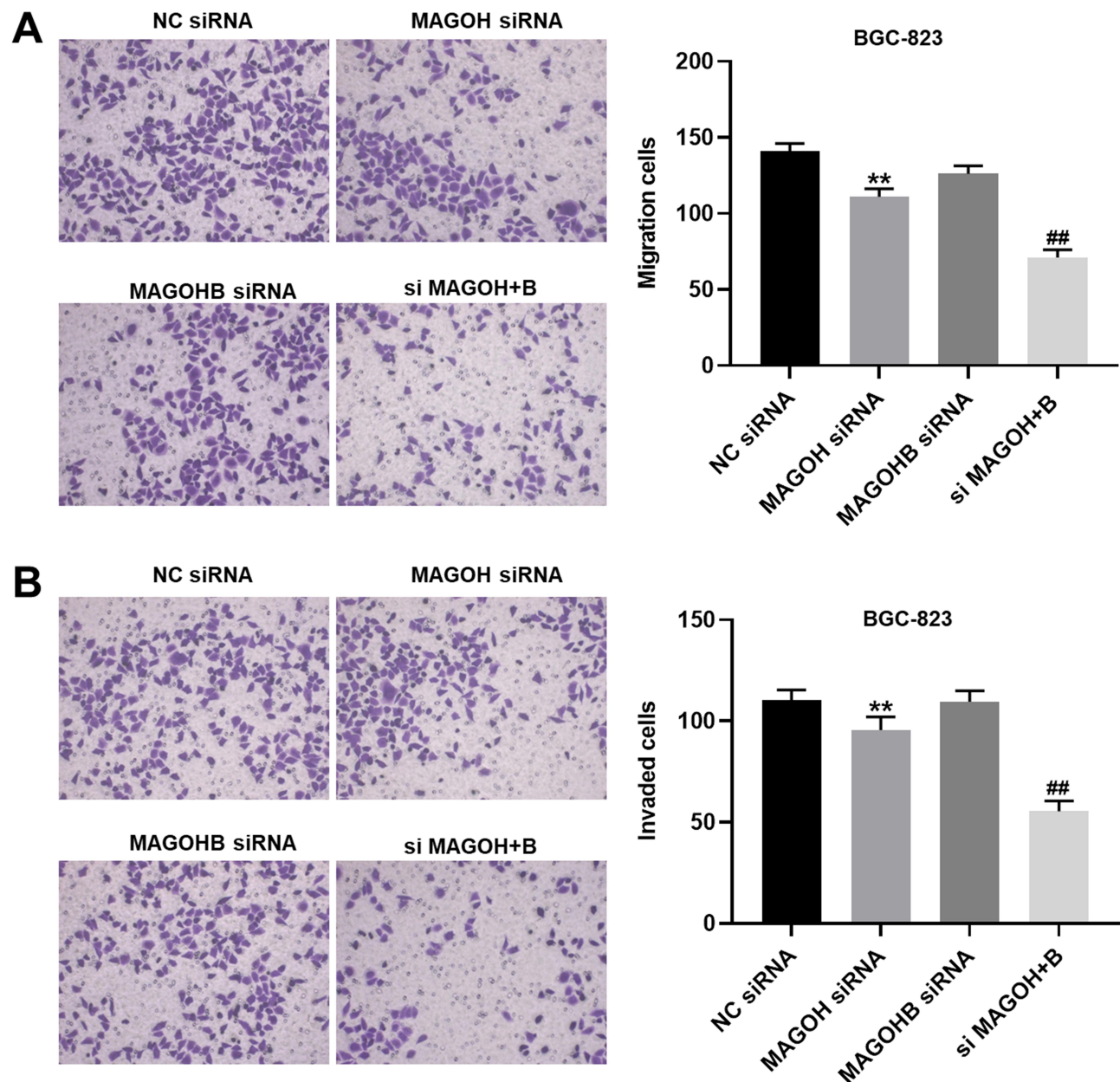
Figure 7 Knockdown of MAGOH or Double Knockdown of MAGOH and MAGOHB notably inhibited the migration and invasion of gastric cancer cells. (**A**) The migration of BGC-823 cells was tested by transwell assay. (**B**) The invasion of BGC-823 cells was tested by transwell assay. **P < 0.01 compared to NC siRNA. ##P<0.01 compared to MAGOH siRNA.

Knockdown of MAGOH or double knockdown of MGOH and MAGOHB Suppressed the Growth of Gastric Cancer Cells by Inducing G2/M Phase Arrest

Next, flow cytometry was performed to detect the cell apoptosis. As shown in Figure 6A, knockdown of MAGOH notably induced the apoptosis of gastric

cancer cells, and the combination treatment triggered much more cell apoptosis. Additionally, knockdown of MAGOH significantly induced G2/M phase arrest in gastric cancer cells (Figure 6B). Interestingly, double knockdown of MAGOH and MAGOHB also induced S phase arrest in gastric cancer cells (Figure 6B). Taken together, double knockdown of MAGOH and MAGOHB suppressed the growth of gastric cancer cells by inducing G2/M phase arrest.
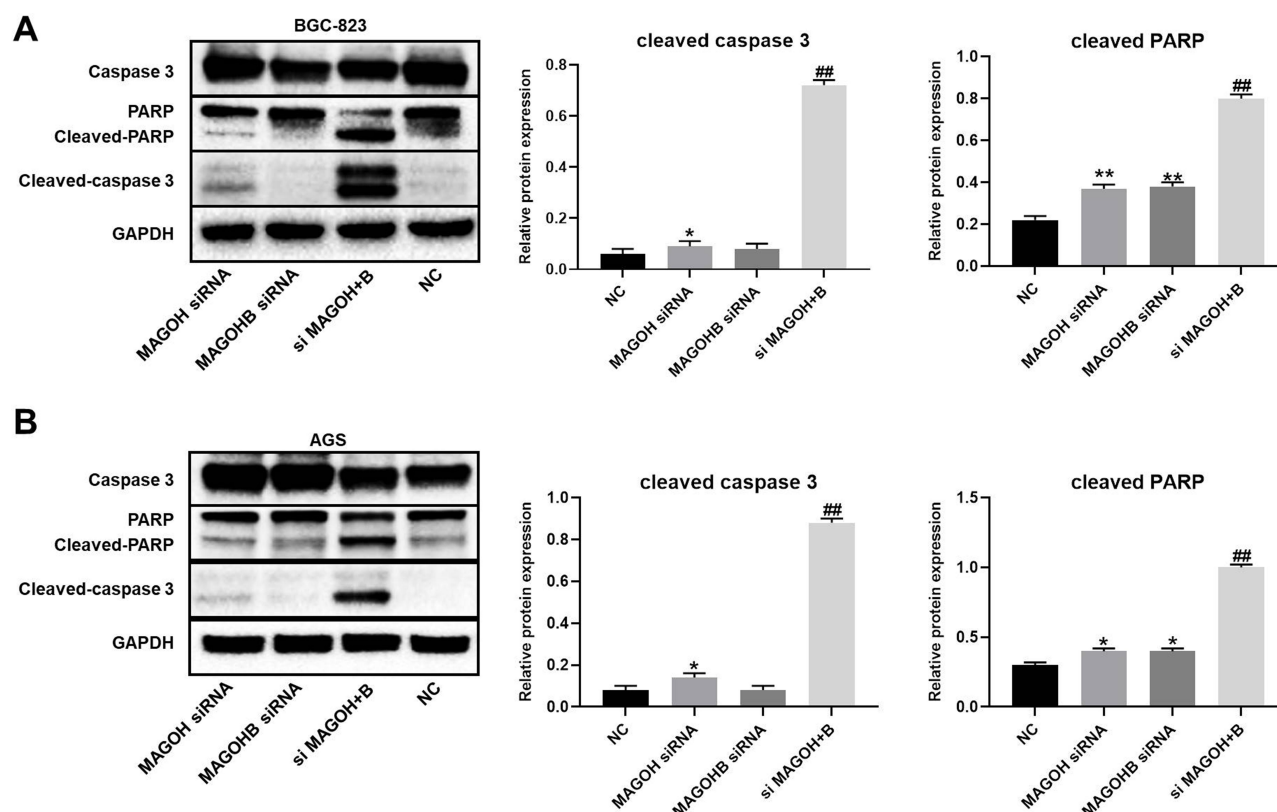
Figure 8 Knockdown of MAGOH or double knockdown of MAGOH and MAGOHB significantly inhibited the growth of gastric cancer cells via upregulation of cleaved caspase 3 and cleaved PARP. (**A**) The protein expressions of PARP, caspase 3, cleaved caspase 3 and cleaved PARP in BGC-823 cells were detected by Western blot. The relative protein expressions were quantified by normalizing to GAPDH. (**B**) The protein expressions of PARP, caspase 3, cleaved caspase 3 and cleaved PARP in AGS cells were detected by Western blot. The relative protein expressions were quantified by normalizing to GAPDH. *P < 0.05, **P < 0.01 compared to NC. ##P< 0.01 compared to MAGOH siRNA.

Knockdown of MAGOH or Double Knockdown of MAGOH and MAGOHB Notably Inhibited the Migration and Invasion of Gastric Cancer Cells

In order to investigate the cell migration and invasion, transwell assay was performed. As revealed in Figure 7A and B, knockdown of MAGOH or double knockdown of MAGOH and MAGOHB significantly inhibited the migration and invasion of gastric cancer cells; the combination exhibited much better anti-migration and anti-invasion effects compared to alone treatment.

Knockdown of MAGOH or double knockdown of MAGOH and MAGOHB Inhibited the Growth of Gastric Cancer Cells via Upregulation of Cleaved Caspase 3 and Cleaved PARP

To investigate the mechanism by which MAGOH or/and MAGOHB knockdown inhibited the growth of gastric cancer cells, Western blot was used. The data revealed

that MAGOH siRNA or MAGOHB siRNA significantly increased the expressions of cleaved caspase 3 and cleaved PARP in BGC-823 cells (Figure 8A and B). Consistently, double knockdown of MAGOH and MAGOHB induced a much more increase of cleaved caspase 3 and cleaved PARP in cells compared with single knockdown (Figure 8A and B). To sum up, knockdown of MAGOH or double knockdown of MAGOH and MAGOHB inhibited the growth of gastric cancer cells via upregulation of cleaved caspase 3 and cleaved PARP.

Double Knockdown of MAGOH and MAGOHB Inhibited the Tumorigenesis of Gastric Cancer via Mediation of b-RAF/MEK/ERK Signaling

Previous report indicated EJC could control the splicing of MAPK that affect MAPK pathway directly.[14] In order to further explore the interaction of MAGOH/MAGOHB and MAPK pathway in gastric cancer, Western blot was performed. As revealed in Figure 9A and B, the expressions of p-RAF and p-MEK in gastric cancer cells were significantly
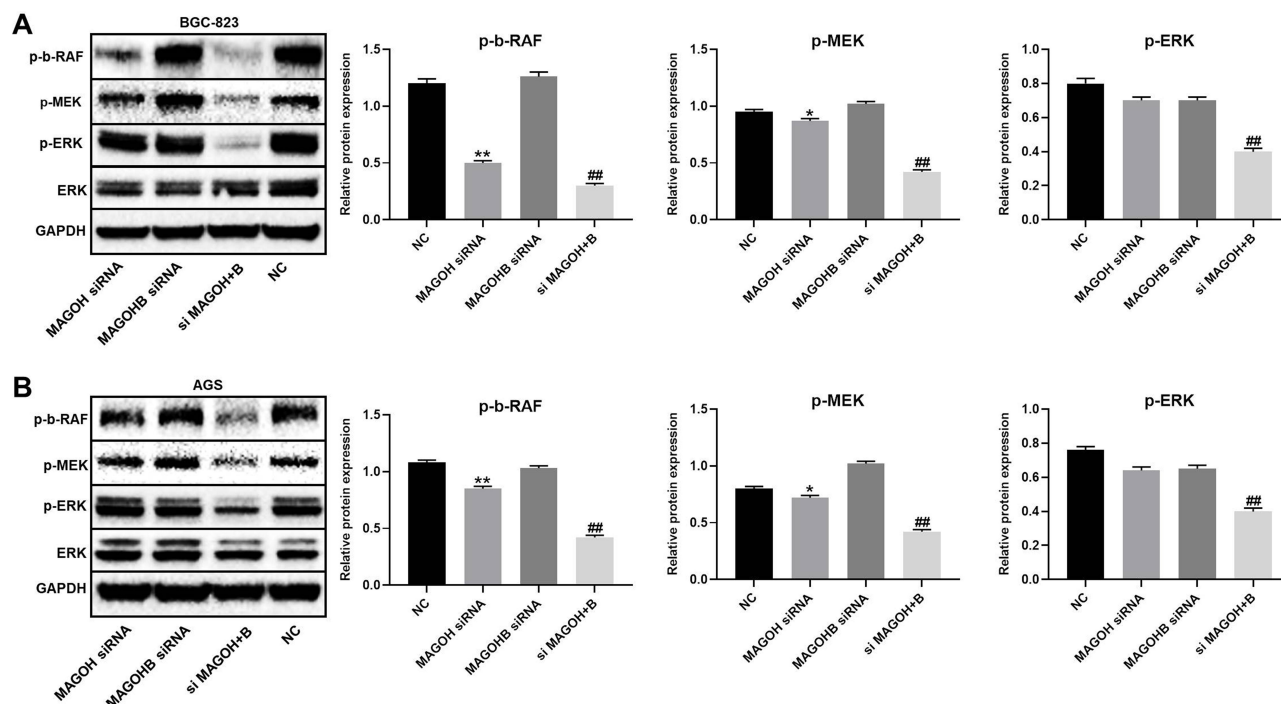
Figure 9 Double knockdown of MAGOH and MAGOHB significantly inhibited the tumorigenesis of gastric cancer via downregulation of RAF/MEK/ERK signaling. (**A**) The protein expressions of p-RAF, p-MEK, ERK and p-ERK in BGC-823 cells were detected by Western blot. The relative protein expressions were quantified by normalizing to GAPDH. (**B**) The protein expressions of p-RAF, p-MEK, ERK and p-ERK in AGS cells were detected by Western blot. The relative protein expressions were quantified by normalizing to GAPDH. *$P < 0.05$, **$P < 0.01$ compared to NC. ##$P < 0.01$ compared to MAGOH siRNA.

downregulated by knockdown of MAGOH or double knockdown of MAGOH and MAGOHB. Consistently, double knockdown of MAGOH and MAGOHB decreased the protein levels of p-RAF, p-ERK and p-MEK much more compared with single knockdown (Figure 9A and B). Taken together, double knockdown of MAGOH and MAGOHB inhibited the tumorigenesis of gastric cancer via mediation of b-RAF/MEK/ERK signaling.

Discussion

Previous studies have indicated that MAGOH and MAGOHB were involved in the progression of breast and prostate cancers.[9,10,15] In this study, we found knockdown of MAGOH or double knockdown of MAGOH and MAGOHB could significantly inhibit the growth of gastric cancer cells. This finding supplemented the biological function of MAGOH and MAGOHB in gastric cancer, further confirming that MAGOH/MAGOHB can act as a key mediator during the tumorigenesis.

It has been confirmed that cleaved caspase 3 and cleaved PARP are important modulators in cell growth.[16–18] Huang et al indicated that cleaved caspase 3 is a pro-apoptotic protein.[19] Additionally, cleaved PARP can also be upregulated during the cell

apoptosis.[20,21] Our finding was consistent with these studies, suggesting that knockdown of MAGOH or double knockdown of MAGOH and MAGOHB induced the apoptosis of gastric cancer cells via upregulation of cleaved caspase 3 and cleaved PARP. Cyclin B1, CDK1 and p27 Kip1 were key mediators in cell cycle distribution.[22–24] Cyclin B1 played a key role in G2/M phase of cell cycle distribution.[25] Downregulation of CDK1 could induce G2/M arrest,[26] while p27 Kip1 was negatively correlated with cell growth.[27] Consistently, our findings revealed that knockdown of MAGOH or double knockdown of MAGOH and MAGOHB affected the cell cycle distribution in gastric cancer via mediation of cyclin B1, CDK1 and p27 Kip1.

In the current study, we found that double knockdown of MAGOH and MAGOHB could inhibit b-RAF/MEK/ERK in gastric cancer cells. B-RAF/MEK/ERK signal pathway mainly contains a three-stage enzyme-linked functional unit, namely RAF, MEK and ERK excitation.[28] Abnormal expression of the b-RAF/MRK/ERK signaling pathway is related with the progression of a number of malignancies.[29–31] In addition, some signaling pathways spread through b-RAF/MEK/ERK in various cellular processes, such as cell growth,

differentiation and apoptosis.[32–34] Our research was consistent with these data, suggesting that double knockdown of MAGOH and MAGOHB inhibited the growth of gastric cancer cells via downregulation of b-RAF/MEK/ERK signaling. Frankly speaking, there is a limitation in this research: This study focused only on RAF/MEK/ERK signaling pathway so far. Thus, more signaling pathways related with cell growth are needed to be investigated in the future.

In conclusion, double knockdown of MAGOH and MAGOHB significantly suppressed the tumorigenesis of gastric cancer via inhibition of b-RAF/MEK/ERK signaling. This finding might provide us a new strategy for the treatment of gastric cancer.

Funding

Disclosure

The authors declared no competing interests in this study. Yong Zhou and Zhongqi Li are co-first authors for this study.

References

1. Arantes V, Uedo N. Polypoid nodule scar after gastric endoscopic submucosal dissection: not so uncommon after resection of neoplasms located in the Antrum. *Digestion*. 2020;1–3. doi:10.1159/000507924
2. Arigami T, Matsushita D, Okubo K, et al. Response rate and prognostic impact of salvage chemotherapy after nivolumab in patients with advanced gastric cancer. *Oncology*;2020;1–7. doi:10.1159/000509530
3. Wan L, Tan N, Zhang N, Xie X. Establishment of an immune microenvironment-based prognostic predictive model for gastric cancer. *Life Sci*. 2020;261:118402. doi:10.1016/j.lfs.2020.118402
4. Yamanaga K, Sakamoto K, Kajiwara I, Tsujita K. Coronary artery perforation into the upper gastrointestinal cavity due to gastric ulceration. *Catheter Cardiovasc Interv*. 2020. doi:10.1002/ccd.28945
5. Suzuki A, Katoh H, Komura D, et al. Defined lifestyle and germline factors predispose Asian populations to gastric cancer. *Sci Adv*. 2020;6 (19):eaav9778. doi:10.1126/sciadv.aav9778
6. Ma Q, Tatsuno T, Nakamura Y, Ishigaki Y. The stability of Magoh and Y14 depends on their heterodimer formation and nuclear localization. *Biochem Biophys Res Commun*. 2019;511(3):631–636. doi:10.1016/j.bbrc.2019.02.097
7. Blazquez L, Emmett W, Faraway R, et al. Exon junction complex shapes the transcriptome by repressing recursive splicing. *Mol Cell*. 2018;72(3):496–509 e499. doi:10.1016/j.molcel.2018.09.033
8. Tatsuno T, Ishigaki Y. C-terminal short arginine/serine repeat sequence-dependent regulation of Y14 (RBM8A) localization. *Sci Rep*. 2018;8(1):612. doi:10.1038/s41598-017-18765-1
9. Viswanathan SR, Nogueira MF, Buss CG, et al. Genome-scale analysis identifies paralog lethality as a vulnerability of chromosome 1p loss in cancer. *Nat Genet*. 2018;50(7):937–943. doi:10.1038/s41588-018-0155-3

10. Stricker TP, Brown CD, Bandlamudi C, et al. Robust stratification of breast cancer subtypes using differential patterns of transcript isoform expression. *PLoS Genet*. 2017;13(3):e1006589. doi:10.1371/journal.pgen.1006589
11. Ladopoulos V, Hofemeister H, Hoogenkamp M, et al. The histone methyltransferase KMT2B is required for RNA polymerase II association and protection from DNA methylation at the MagohB CpG island promoter. *Mol Cell Biol*. 2013;33(7):1383–1393. doi:10.1128/MCB.01721-12
12. Singh KK, Wachsmuth L, Kulozik AE, Gehring NH. Two mammalian MAGOH genes contribute to exon junction complex composition and nonsense-mediated decay. *RNA Biol*. 2013;10(8):1291–1298. doi:10.4161/rna.25827
13. Azim HA, Peccatori FA, Brohee S, et al. RANK-ligand (RANKL) expression in young breast cancer patients and during pregnancy. *Breast Cancer Res*. 2015;17:24.
14. Ashton-Beaucage D, Udell CM, Lavoie H, et al. The exon junction complex controls the splicing of MAPK and other long intron-containing transcripts in Drosophila. *Cell*. 2010;143 (2):251–262. doi:10.1016/j.cell.2010.09.014
15. Dong YM, Li M, He QE, et al. Epigenome-wide tobacco-related methylation signature identification and their multilevel regulatory network inference for lung adenocarcinoma. *Biomed Res Int*. 2020;2020:2471915. doi:10.1155/2020/2471915
16. Ali FEM, Hassanein EHM, Bakr AG, et al. Ursodeoxycholic acid abrogates gentamicin-induced hepatotoxicity in rats: role of NF-kappaB-p65/TNF-alpha, Bax/Bcl-xl/Caspase-3, and eNOS/iNOS pathways. *Life Sci*. 2020;254:117760. doi:10.1016/j.lfs.2020.117760
17. Liu MM, Dong R, Hua Z, et al. Therapeutic potential of Liuwei Dihuang Pill against KDM7a and Wnt/beta-catenin signaling pathway in diabetic nephropathy-related osteoporosis. *Biosci Rep*. 2020;40(9). doi:10.1042/BSR20201778.
18. Li M, Xue Y, Yu H, Mao D. Quercetin alleviated H2 O2 -induced apoptosis and steroidogenic impairment in goat luteinized granulosa cells. *J Biochem Mol Toxicol*. 2020;e22527.
19. Huang D, Peng Y, Ma K, et al. Puerarin relieved compression-induced apoptosis and mitochondrial dysfunction in human nucleus pulposus mesenchymal stem cells via the PI3K/Akt pathway. *Stem Cells Int*. 2020;2020:7126914. doi:10.1155/2020/7126914
20. Liu H, Guo H, Jian Z, et al. Copper induces oxidative stress and apoptosis in the mouse liver. *Oxid Med Cell Longev*. 2020;2020:1359164.
21. Liu HC, Chiang CC, Lin CH, et al. Anti-cancer therapeutic benefit of red guava extracts as a potential therapy in combination with doxorubicin or targeted therapy for triple-negative breast cancer cells. *Int J Med Sci*. 2020;17(8):1015–1022. doi:10.7150/ijms.40131
22. Ma J, Zhang Y, Deng H, et al. Thymoquinone inhibits the proliferation and invasion of esophageal cancer cells by disrupting the AKT/GSK-3beta/Wnt signaling pathway via PTEN upregulation. *Phytother Res*. 2020. doi:10.1002/ptr.6795
23. Guan X, Guan Y. Artemisinin induces selective and potent anticancer effects in drug resistant breast cancer cells by inducing cellular apoptosis and autophagy and G2/M cell cycle arrest. *J BUON*. 2020;25(3):1330–1336.
24. Zou Y, Ruan S, Jin L, et al. CDK1, CCNB1, and CCNB2 are prognostic biomarkers and correlated with immune infiltration in hepatocellular carcinoma. *Med Sci Monit*. 2020;26:e925289. doi:10.12659/MSM.925289
25. Yao M, Li R, Yang Z, et al. PP9, a steroidal saponin, induces G2/M arrest and apoptosis in human colorectal cancer cells by inhibiting the PI3K/Akt/GSK3beta pathway. *Chem Biol Interact*. 2020;331:109246. doi:10.1016/j.cbi.2020.109246
26. Willis L, Jonsson H, Huang KC. Limits and constraints on mechanisms of cell-cycle regulation imposed by cell size-homeostasis measurements. *Cell Rep*. 2020;32(6):107992. doi:10.1016/j.celrep.2020.107992

27. El-Daly SM, Gamal-Eldeen AM, Gouhar SA, Abo-Elfadl MT, El-Saeed G. Modulatory effect of indoles on the expression of miRNAs regulating G1/S cell cycle phase in breast cancer cells. *Appl Biochem Biotechnol*. 2020. doi:10.1007/s12010-020-03378-8

28. Du Y, Zhang MJ, Li LL, et al. ATPR triggers acute myeloid leukaemia cells differentiation and cycle arrest via the RARalpha/LDHB/ERK-glycolysis signalling axis. *J Cell Mol Med*. 2020;24 (12):6952–6965. doi:10.1111/jcmm.15353

29. Deng D, Yang S, Wang X. Long non-coding RNA SNHG16 regulates cell behaviors through miR-542-3p/HNF4alpha axis via RAS/RAF/MEK/ERK signaling pathway in pediatric neuroblastoma cells. *Biosci Rep*. 2020;40(5). doi:10.1042/BSR20200723

30. Bertrand FE. The cross-talk of NOTCH and GSK-3 signaling in colon and other cancers. *Biochim Biophys Acta Mol Cell Res*. 2020;1867(9):118738. doi:10.1016/j.bbamcr.2020.118738

31. Yoshitake R, Saeki K, Eto S, et al. Aberrant expression of the COX2/PGE2 axis is induced by activation of the RAF/MEK/ERK pathway in BRAF(V595E) canine urothelial carcinoma. *Sci Rep*. 2020;10 (1):7826. doi:10.1038/s41598-020-64832-5

32. Hasinoff BB, Patel D. Mechanisms of the cardiac myocyte-damaging effects of dasatinib. *Cardiovasc Toxicol*. 2020;20(4):380–389. doi:10.1007/s12012-020-09565-7

33. Zhang D, Yang Y, Li Y, Zhang G, Cheng Z. Inhibitory effect of curcumin on artery restenosis following carotid endarterectomy and its associated mechanism in vitro and in vivo. *Drug Des Devel Ther*. 2020;14:855–866. doi:10.2147/DDDT.S229607

34. Guo J, Lan Z. Expression of concern: PHD2 acts as an oncogene through activation of Ras/Raf/MEK/ERK and JAK1/STAT3 pathways in human hepatocellular carcinoma cells. *Artif Cells Nanomed Biotechnol*. 2020;48(1):712. doi:10.1080/21691401.2020.1741861